GTX REFERENCE VEHICLE STRUCTURAL VERIFICATION METHODS AND WEIGHT SUMMARY

J.E. Hunter
National Aeronautics and Space Administration
Glenn Research Center
Cleveland, Ohio 44135

D.R. McCurdy
QSS Group, Inc.
Cleveland, Ohio 44135

P.W. Dunn
National Aeronautics and Space Administration
Glenn Research Center
Cleveland, Ohio 44135

ABSTRACT

The design of a single-stage-to-orbit air breathing propulsion system requires the simultaneous development of a reference launch vehicle in order to achieve the optimal mission performance. Accordingly, for the GTX study a 300-lb payload reference vehicle was preliminarily sized to a gross liftoff weight (GLOW) of 238,000 lb. A finite element model of the integrated vehicle/propulsion system was subjected to the trajectory environment and subsequently optimized for structural efficiency. This study involved the development of aerodynamic loads mapped to finite element models of the integrated system in order to assess vehicle margins of safety. Commercially available analysis codes were used in the process along with some internally developed spreadsheets and FORTRAN codes specific to the GTX geometry for mapping of thermal and pressure loads. A mass fraction of 0.20 for the integrated system dry weight has been the driver for a vehicle design consisting of state-of-the-art composite materials in order to meet the rigid weight requirements. This paper summarizes the methodology used for preliminary analyses and presents the current status of the weight optimization for the structural components of the integrated system.

INTRODUCTION

The NASA approach to advance access to space is a program consisting of three phases. The third phase, known as Generation 3, includes development of revolutionary propulsion technology. NASA Glenn Research Center (GRC) has been developing Rocket-Based Combined-Cycle (RBCC) propulsion as a means to achieve this goal. GRC believes that for Single-Stage-to-Orbit (SSTO) to become feasible, the propulsion system must be fully integrated to a reference vehicle concept and concurrently developed. This approach lends itself to optimization at the highest possible level of the system including trajectory considerations. Consequently, the GTX concept was selected as a candidate integral propulsion/vehicle system of high optimization potential. Pratt & Whitney is an industry partner providing expertise in the area of propulsion system architecture and thermal management.[1]

The GTX vehicle concept would launch from sea level static conditions and accelerate to hypersonic speed while in the earth's atmosphere. The aerodynamic environment, both pressure and heating, could be very severe in the air-breathing segment of the trajectory. To reduce the impact of this environment, a high thrust-to-weight vertical take-off mission profile was selected. This effectively shortens the mission, minimizes aero-heating and keeps the vehicle weight to a minimum.

Meeting the aggressive goals of SSTO necessitates the use of advanced composite materials that meet the requirements for environment and strength. Near term material systems have been selected for the initial assessment of the GTX design. None-the-less, those materials selected for this magnitude of application must be continuously developed in order for a Generation 3 SSTO vehicle to be successful.

The purpose of this paper is to explain the steps taken for an early engineering assessment of the GTX integrated propulsion/vehicle system. This encompasses the initial design effort to target a reference vehicle and subsequent analyses with a focus on optimization for weight. The achievement of this ambitious goal will require several iterations. This paper summarizes the status of work done up to the present time along with the current weight status.

Approved for public release, distribution is unlimited.

RESULTS AND DISCUSSION

GTX DESIGN REQUIREMENTS

All design requirements for GTX as an integrated single-stage-to-orbit (SSTO) vehicle are derived to maximize the use of air breathing performance while minimizing structural weight. GTX is designed as a vertical take-off and horizontal landing concept in order to minimize wing and landing gear structure. As a design requirement, this should reduce the reliance on aerodynamics at low speed.[2] Sharp leading edges on the nosetip, wings, tail, and cowl are required in order to reduce vehicle drag, especially at hypersonic speeds. The propellant requirements are liquid oxygen (LOX) and liquid hydrogen (LH2) selected for energy per unit mass advantage as well as for cooling properties. While the GTX is to be reusable, the number of missions the vehicle is to be capable of flying has not been specified at this point in the study. A 300-lb payload has been specified for initial structural assessments with an emphasis on bringing the integrated vehicle system to closure. A mission profile (trajectory) is required to establish critical flight environments and may have constrictions applied to offset excessive loading of the system. For example, the angle of attack at the end of the scramjet phase was limited to six degrees so that aerodynamic loads do not increase the system weight. Requirements allow for scaling of the integrated vehicle to achieve greater payload capability and/or reach the ultimate goal of vehicle closure. These basic requirements and the need for structural efficiency led to the design of a reference vehicle concept.

REFERENCE VEHICLE CONCEPT

The basic vehicle configuration is pictured in Figure 1. The three propulsion pods are placed 120 degrees apart and symmetric about a vertical plane thru the tail. A cut-away view of the RBCC engine structure is shown in Figure 2. It consists of a cowl, which provides the flow path geometry, a translating centerbody, which controls air inlet, and a diverter pad, which diverts the boundary layer air from the engine inlet. Inside the cowl a rocket element is mounted just aft of the centerbody to provide the thrust during those flight events where air is not captured at the inlet. The engine cowl architecture consists of an outer skin supported by ring and stringer frame structure within. On the hot side of the cowl frame structure, a heat exchanger with corrugated backup structure makes up the engine liner.

The vehicle nose/fuselage skin panels are stiffened by an internal frame structure consisting of rings and stringers. The aero shell skin panels are comprised of a sandwich section that has a carbon foam core and Carbon/Silicone-Carbide face sheets. C/SiC was selected for its oxidation resistance under the harsh environment during flight. The nose would be built with jointed segments along the axis of the vehicle for ease of manufacturing and assembly. The preferred material for internal frame members is carbon-carbon beam sections with an optimized ply lay-up for strength and stiffness.

The engine liner/heat exchanger panels are directly supported off the fuselage rings. A sketch of the heat exchanger and supporting structure is shown in Figure 3. The preliminary heat exchanger material used in this assessment is a C/SiC design with closely spaced cooling passages. The heat exchanger panels are primarily designed to take temperature and pressure loads while the back-up stiffening structure (i.e., integral hat section beams) is designed to react both pressure load and other structure-born loads within the liner.

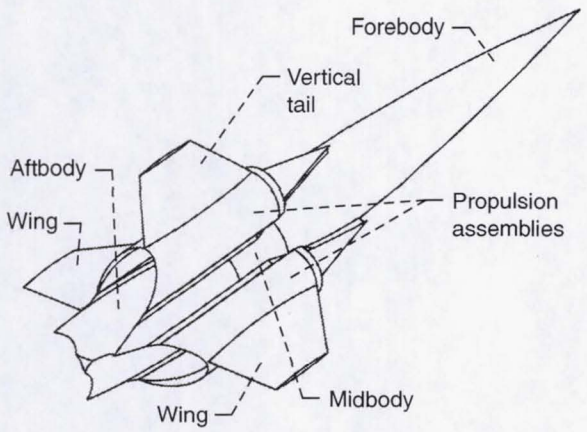

Figure 1.—Vehicle configuration.

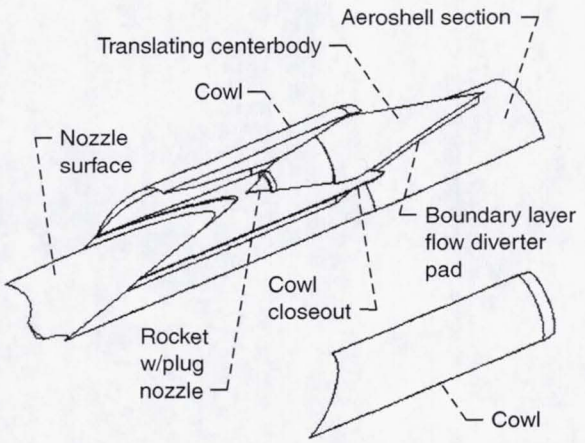

Figure 2.—GTX propulsion system cut-away view.

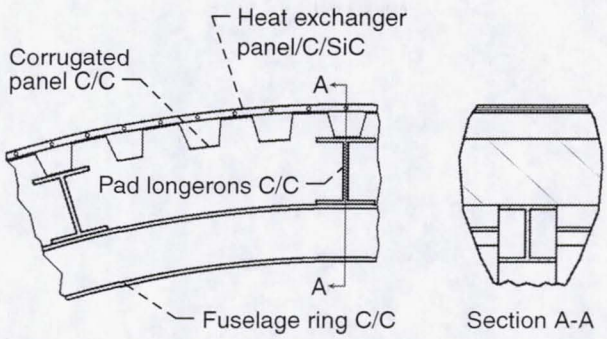

Figure 3.—Sketch of heat exchanger and supporting structure.

The engine cowl and wings are designed with sharp leading edges for reduced drag. Material for these leading edges is a high conductivity 3d carbon-carbon with an oxidation resistant coating. This material/coating system was selected for the diverter pad and centerbody leading edge, as well. The cowl/wing skin section is similar to that used for the nose/fuselage skin panels and has a 1.0 inch carbon foam core with 0.05 inch C/SiC face sheets.

The propellant tanks were designed with a circular cross section for optimal structural efficiency. The tanks also conform to the shape of the nose/fuselage along the longitudinal axis for volumetric efficiency. The annulus between the tank shell and outer vehicle skin provides space for fuselage ring and stringer members and thermal insulation. A graphite/epoxy general grid construction was selected for the cryogenic tank designs. The tank thermal protection system (TPS) consists of a thin layer of saffil foam covered by multi-layer insulation.

After defining the reference vehicle concept, the next step was to determine its preliminary size.

PRELIMINARY SIZING

The reference size of a closed vehicle for a given mission trajectory depends on engine performance, the weight and size of structure and equipment, and volumetric efficiency of fuel stowage. GTXSizer,[3] a spreadsheet tool that synthesizes a vehicle capable of meeting the mission requirements, has been developed at GRC for the purpose of proportionally scaling the geometry and structural weight to a size that indicates closure. Closure is defined as that size where the propellant fraction available (PFA) meets or exceeds the propellant fraction required (PFR). Establishing a reference vehicle for closure involves some iteration between the spreadsheet execution and trajectory analyses using the Optimal Trajectory by Implicit Simulation (OTIS) software[4] with a consistent set of performance parameters.

Prior to the development of GTXSizer, an initial GTX reference vehicle design was based on the preliminary weight study of vehicle components taken from data of historical NASA programs as well as of methods from reference 5. Structural analysis was then performed on this smaller scale version to verify those weights and provide a basis for any future scaling that may be necessary to achieve a closed vehicle. Structural weights and scaling of vehicle acreage areas were evaluated based on the ability of the structure to withstand the mechanical and thermal loads throughout the flight. Analysis verified that the initial vehicle size was insufficient to achieve closure. Lessons learned from this study, however, brought about some important design and material changes. Also, the area densities were modified and incorporated into the spreadsheet for an improved accuracy in scaling a future reference vehicle.

Subsequent to that, results of the reference vehicle scaling established a preliminary gross liftoff weight (GLOW) of 238,200 pounds as the baseline used for this analysis iteration. The corresponding vehicle dry weight allowance including payload was 41,500 pounds.

METHODS AND TECHNICAL APPROACH

After establishing a reference vehicle size and target GLOW, the next step was to provide a set of layout drawings to be used in the structural assessment. A solid model was made for the GTX configuration using a computer aided design tool, Pro/ENGINEER® (Pro/E).[6] One important feature built into the solid model was the capability to scale the geometry based on the input of a few specific dimensions, namely body radius, vehicle length, and nose tip to engine cowl lip length. These key dimensions were part of the output from the spreadsheet sizing tool (GTXSizer).

Subsequently, the key dimensions for the scaled up reference vehicle were plugged into Pro/E resulting in a new set of geometric dimensions, as shown in Figure 4. The dimensioned drawings were used to create a model in Aerodynamic Preliminary Analysis System (APAS) code[7] of the outer mold line (OML) for aerodynamic analyses. Lift and drag information from APAS was used iteratively with OTIS in order to converge on vehicle closure. After closure was confirmed for the target GLOW of 238,200 pounds, the trajectory was reviewed in order to define the critical load events. The focus of this step was to select those cases for static analysis, which had the potential to drive the design.

This process leading up to the investigation and the ensuing analytical approach is shown by the flow chart in Figure 5. Structural assessment was made using both a propulsion system fine mesh analysis and a coarsely meshed mass stiffness model of the fully integrated vehicle for the critical environments. The purpose of the coarse mesh model was to assess the overall integrated vehicle system behavior due to flight environments while the detailed engine finite element model (FEM) was concentrated more toward propulsion system architecture with structural weight implications.

INTEGRATED VEHICLE FINITE ELEMENT MODEL

Once closure had been established, the OML nodes from the APAS model were imported into the finite element processing code, MSC/PATRAN™ (ref. 8) and these nodes were in essence duplicated for the FEM aero surface mesh. This one-to-one node match was advantageous for mapping APAS aero loads to the vehicle skin or wetted surface. Other structure was then incorporated into the integrated vehicle FEM (see fig. 6) such as the flow path liner panels inside the engine cowls. The engine cowl rings and stringers were modeled as bar elements offset between the aero shell surface and the liner panels. Wing skin panels were modeled as plate elements, internal bars represented the spars, and ribs were modeled as plate elements. Wing spars connected rigidly into the cowl rings that are attached to fuselage rings thereby providing a continuous load path to react wing aerodynamic pressure loads.

The vehicle fore-body is comprised of an aeroshell composite skin modeled as sandwich plate elements and supported by the internal rings and stringers, which are modeled as bars with offsets. The propellant tank walls are modeled as 2D anisotropic shell elements. The conical tank adapter is modeled similarly but with ring and stringer stiffeners for added stiffness. The tank/adapter assembly is supported by the fuselage/nose only at discrete locations as shown in Figure 7. The propellant tank assembly is supported axially and laterally at point b, which is a primary thrust ring for engine loads. The propellant tank assembly is laterally supported at two other stations as shown. This support method alleviates high stresses as a result of differential expansion between the cryogenic tanks and the aero shell of the vehicle.

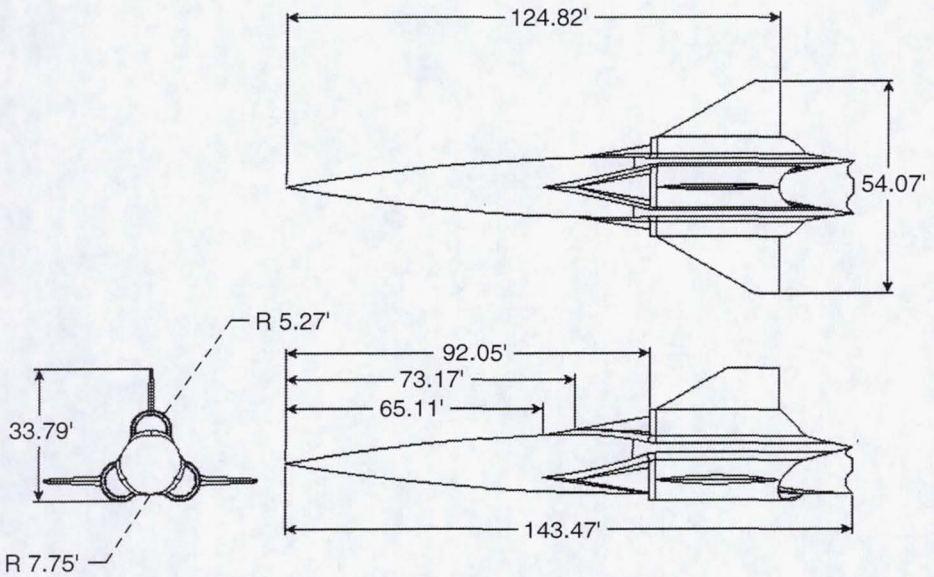

Figure 4.—GTX reference vehicle layout.

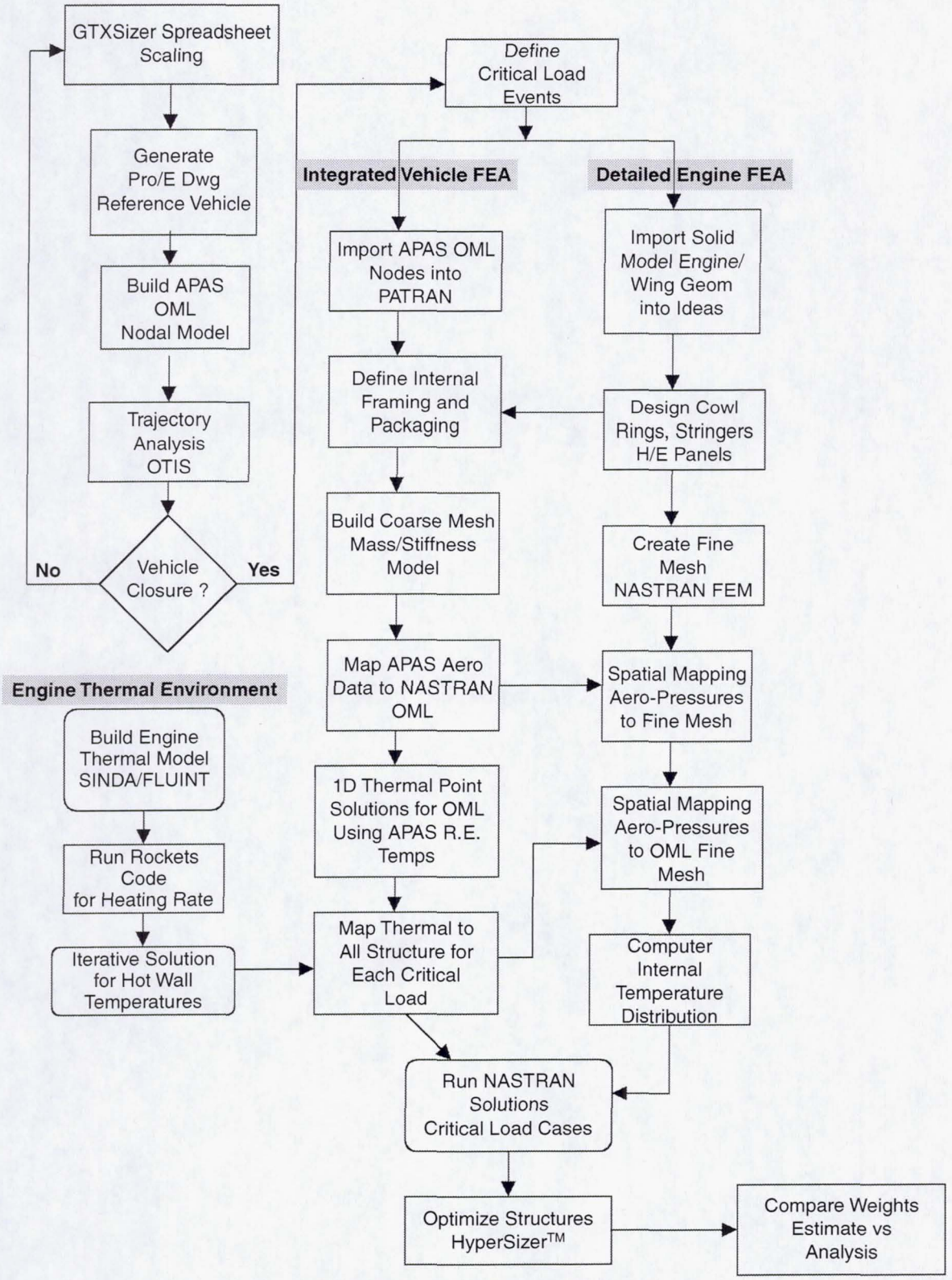

Figure 5.—Technical evaluation process flow chart.

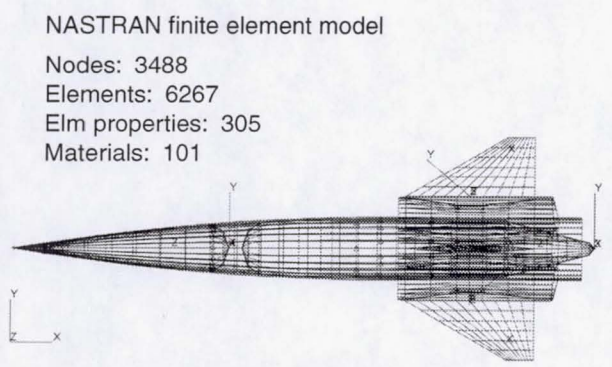

Configuration 10a

Figure 6.—Integrated vehicle finite element model.

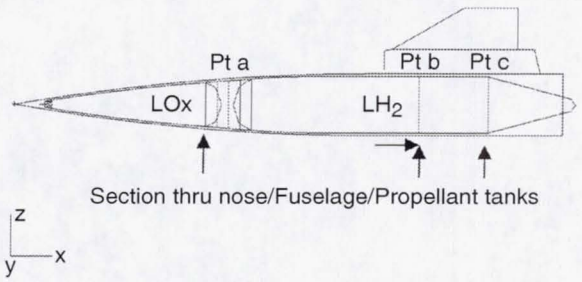

Figure 7.—Propellant tank interface constraints.

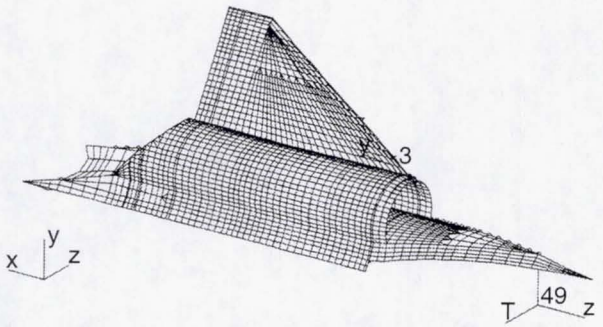

Figure 8.—Detailed engine finite element model.

Flight equipment weights as predicted by GTXSizer, including avionics, hydraulics, and landing gear, are added to the integrated vehicle FEM using distributed or point mass elements as appropriate. Some of the mass and member property data for engine structure is obtained from the detailed engine analysis, which was performed in parallel with the integrated vehicle analysis. The engine exit nozzle was not precisely modeled in the integrated FEM since weight estimations for this region would be forthcoming from the detailed analysis of the engine. Boundary conditions for the integrated vehicle assessment were accomplished using methods of *Inertia Relief* which are capabilities within the MSC/NASTRAN finite element code.[9] This method effectively balances the applied loads about a point near the vehicle center of gravity simulating a vehicle in flight.

DETAILED ENGINE FINITE ELEMENT MODEL

The development of a propulsion system finite element model started with the precise geometry definition as obtained from the solid model. This geometry included the surface definitions of the cowl outer mold line, diverter pad, exit nozzle and engine liner. Since the starboard engine was selected, surface of the wing attached at the cowl was also included. Incorporating the wing into the model permitted a greater accuracy in applying wing loads at the cowl interface. Figure 8 shows and isometric view of the propulsion system FEM.

The cowl outer skin, similar to the vehicle nose, was modeled as composite sandwich panels represented with plate elements in NASTRAN. The wing skins, both top and bottom, were represented in the same way. All sharp leading edges, however, were modeled using solid elements. The wing spars and ribs were modeled with plate elements using an equivalent orthotropic material to represent the composite ply beam sections. A preliminary hand analysis was done to provide the initial input properties for the major load carrying members.

Internal structure for the cowl was modeled in similar fashion to the wing members and consisted of bulkheads and stringers. The semi-circular bulkheads were initially designed manually and served as load path members to transfer wing loads into the fuselage structure. The liner panels consisted of heat exchanger shell with backup stiffening structure all modeled as a built up plate section. The equivalent properties for the built up section were established using HyperSizer™ (ref. 10), a software tool, which automates the methods for structural assessment

and design optimization for a variety of plate and beam designs. Some variation in panel properties was selected due to a variable pressure profile along the engine axis.

The sliding centerbody was represented only as a point mass element, since its stiffness does not contribute to the overall fuselage or engine stiffness. Additional mass elements represented the landing gear, hydraulic systems, fuel feed components, and reaction control systems. Magnitudes of the equipment masses were predicted by GTXSizer.

Boundary conditions were accounted for by incorporating a 120-degree segment of the fuselage and exit nozzle into the FEM. This extension permitted some flexibility at the cowl to fuselage interface as would be expected in the fully integrated vehicle system.

CRITICAL LOAD DETERMINATION

Selection of the critical loads for the integrated vehicle structure assessment was made after a careful review of the ascent trajectory. A total of five critical events were selected (see fig. 9) for investigation of the ascent trajectory ranging from Liftoff to mach 11. The intent was to bound the worse case environment for each system by the combining of inertial loads, aerodynamic pressures and temperatures, and internal combustion effects at each critical load event. The first critical event was that of liftoff since the propellant tanks are at full capacity and will experience high inertia loads along with the tank interface structure at the fuselage. The next critical event occurs at mach 2.5 when the rocket engine is shut down just prior to the ramjet phase. The third critical event occurs at the end of the ramjet phase near mach 5. At this event, the internal combustion pressures have reached the peak levels during ascent. The fourth critical load event selected was at mach 10 where aero heating has become critical to the outer shell of the integrated vehicle. Finally, mach 11 was selected as critical since aero heating is at a peak and the trajectory angle of attack is at six degrees as the vehicle turns up for the coast to orbit. These five cases were thus selected as points in the trajectory where loads would be combined in order to bound the problem for design of all vehicle systems. Other cases were looked at for local structure such as impact loads at landing and peak wing loads at mach 0.8 but the full set of simultaneous loads were not developed for these conditions.

For the finite element assessment of the detailed propulsion system, the three critical cases selected were liftoff, mach 5 and mach 11, since these would most likely be the design drivers for the engine structure.

The determination of critical load cases to be considered in the FEM solutions was followed by a comprehensive definition of the environments for the affected structure.

Mach number	Total acceleration	Axial acceleration	Normal acceleration
0	1.67g	1.67g	0.00g
2.5	1.39g	1.30g	0.49g
5	1.48g	1.31g	0.69g
10	0.89g	0.46g	0.75g
11	0.75g	0.23g	0.72g

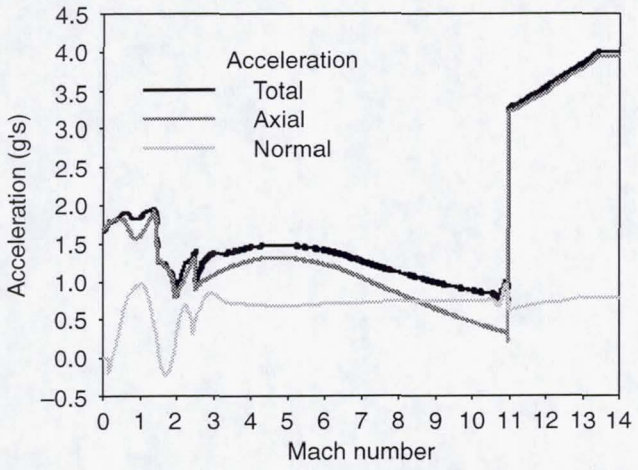

Figure 9.—Acceleration versus Mach no/critical load events.

AERODYNAMIC PRESSURE MAPPING

The aerodynamic pressure coefficients were obtained from APAS at the centroid of each node group. A FORTRAN code was written to convert the coefficients into pressure (psi) units for a corresponding finite element in the PATRAN™ model and to write a full set of NASTRAN™ load cards for the externally applied pressures. The aerodynamic pressures then were mapped for each critical load set over the outer mold line surface of the integrated vehicle FEM. Since the fine mesh engine/wing assembly model had a similar OML envelope, the pressures could then be mapped from the coarse to the fine mesh OML. This was accomplished in PATRAN™ using the *spatial field* method to transfer loads from one model to the other.

AERODYNAMIC THERMAL ANALYSIS (POINT SOLUTIONS)

APAS temperature output consists of the radiation equilibrium temperature (RET) at the centroid of each node group. The RET represents the steady state temperature that an adiabatic surface would experience as a result of convective aerodynamic heat input and surface radiation output. While the calculation of the RET provides an estimate of vehicle surface temperatures, it does not account for heat conduction into the vehicle structure and, thus, provides no information on the in-depth structural temperatures. Therefore, it was necessary to devise a method of preliminary thermal analysis that would take into account the transient effects of heat transfer between the outer skin surface and inboard structure. This was accomplished by developing one-dimensional thermal models at selective points along the nose, cowl, wing, and tail sections. The one-dimensional thermal models were created using SINDA/FLUINT[11] software codes. A typical cross-section for SINDA modeling of the vehicle fore-body that surrounds the cryogenic propellant tank is shown in Figure 10. Similarly, one-dimensional models of the cowl section represented structure from the outer skin surface down to the heat exchanger.

The aerodynamic heating rates were computed by MINIVER[12] and were used as surface boundary conditions for the one-dimensional thermal models. MINIVER uses standard engineering techniques to compute the local flowfield and heating rates over basic airframe shapes, such as nose tip stagnation areas, windward centerline and acreage areas for conical or wedge geometries, and wing/tail leading edges. The code was used to compute the aerodynamic heating rates (boundary layer recovery temperature and convective film coefficient) at selected locations on the nose, cowl, wing, and tail sections. These single point solutions were used to gain insight into the temperature versus time relationships between skin surface and internal structure.

Finally, plots of the temperature versus time were made for each of the thermal point solutions as shown by the example in Figure 11. This plot, at station X = 492 along the vehicle nose, shows the time lag for thermal heating of the outer face sheet and the structural ring frame inside the nose. Also, a transient thermal gradient can be seen for the skin sandwich panel between the inner and outer face sheets. A representative number of one-dimensional thermal point solutions were analyzed for all the major vehicle systems to understand the pattern of behavior during the ascent trajectory. Only the acreage areas of the vehicle were investigated, leaving the detailed regions such as nose tip, wing/tail leading edges, and areas of localized heating amplification, such as shock impingement, for future analyses.

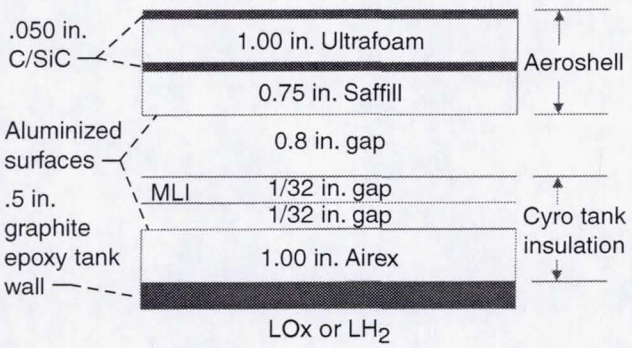

Figure 10.—Typical cross-section for SINDA model.

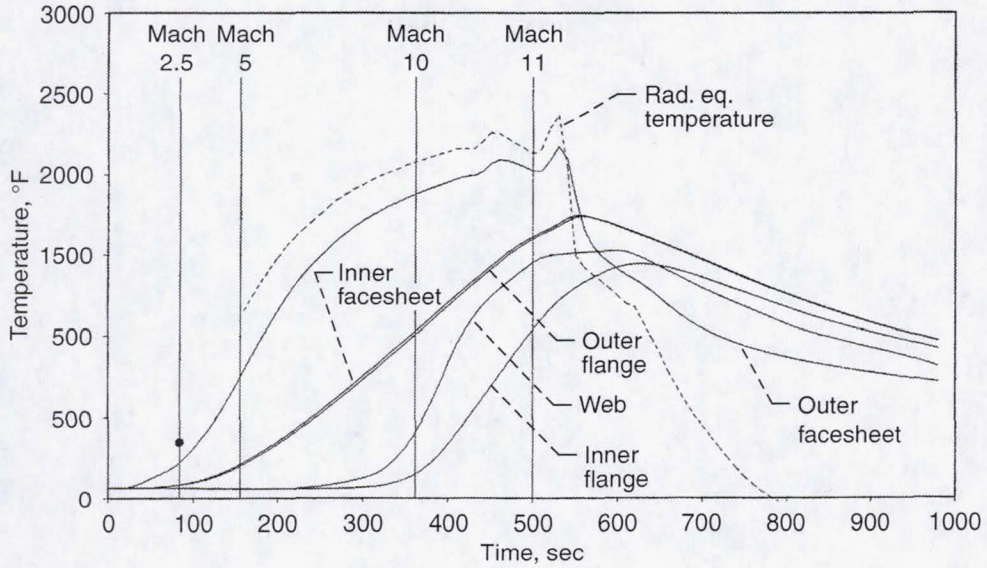

Figure 11.—Thermal point solution at vehicle nose station X = 492.

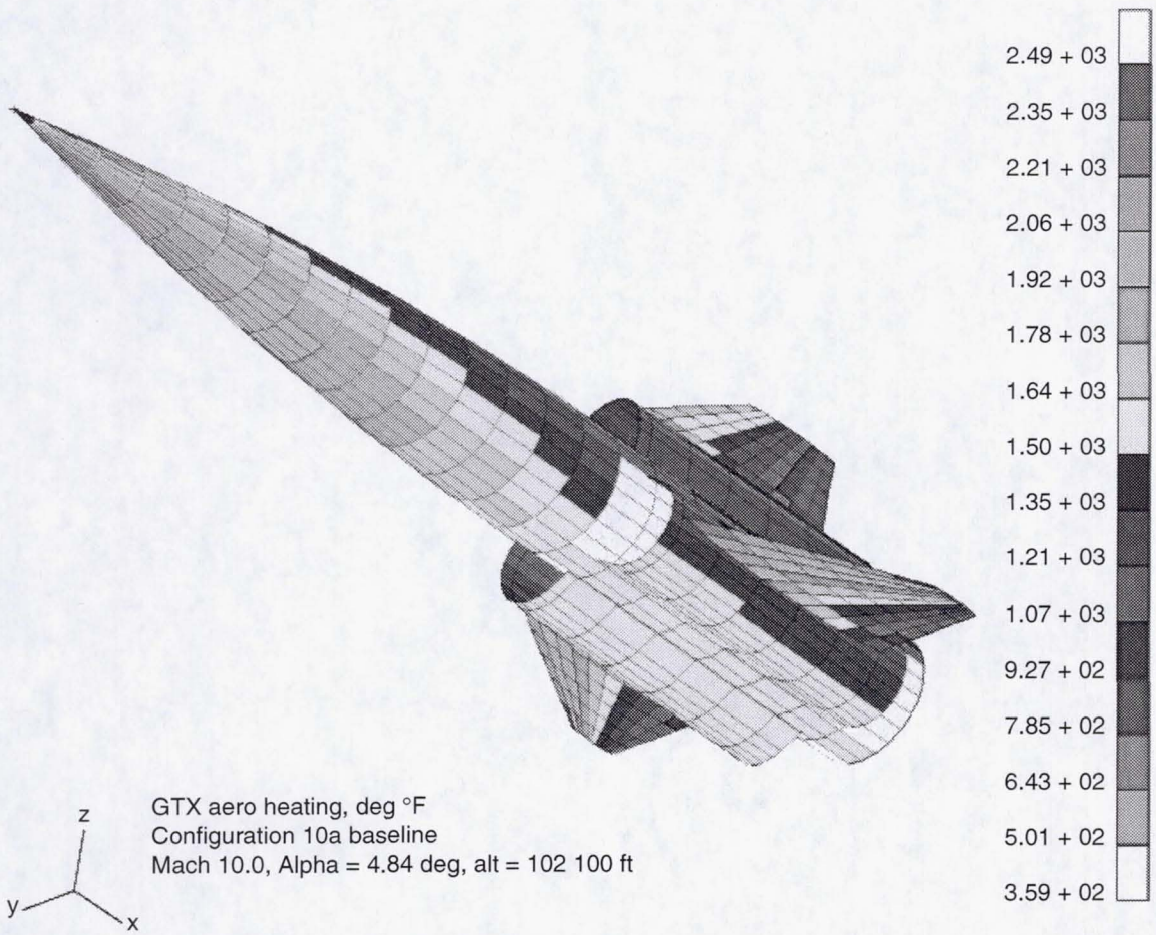

Figure 12.— Vehicle skin thermal map for Mach 10 case.

AERODYNAMIC THERMAL MAPPING

Since it was not feasible to generate thermal point solutions for all gridpoints on the integrated vehicle FEM, it was assumed that the structure near those areas where point solutions were available behaved in a similar manner. Thus, the thermal point solutions provided the relationship between the RET, the actual skin temperature, and substructure temperature. For each primary assembly of the nose, fuselage, cowl, wing, and tail, temperatures were mapped over the complete integrated vehicle FEM. This process was automated with a custom FORTRAN code tailored for the GTX integrated vehicle FEM. The FORTRAN code was used to read RET for each surface element in the integrated vehicle FEM, apply a respective factor to the RET in order to compute internal and external temperatures, and generate a set of temperature load cards formatted for use in NASTRAN. A full set of thermal load cards was generated in this way for each of the ascent cases used in this investigation. A mapping of the mach 10 case for aero heating of the external vehicle skin is shown in Figure 12.

The surface mapped temperatures for those load cases applicable to the detailed engine FEM were then imported and mapped to the fine mesh model using the *spatial field* technique in PATRAN™. The thermal mapping of the internal rings and spars of the detailed model required additional analysis since the detailed model used shell elements instead of bars. The temperature distribution for the interior members, including cowl rings, cowl stringers, wing ribs, and wing spars, was determined using their average temperatures and the outside surface temperatures for the upper and lower cowl and wing skins. Given the upper and lower temperatures of a beam web along with its average temperature, the distribution through the web was approximated by assuming a parabolic distribution. Another custom FORTRAN program was created to map those temperatures through the depth of the rings and bulkheads.

INTERNAL ENGINE ENVIRONMENT

Maintaining temperatures within the material limits of the engine flowpath liner was accomplished with liquid hydrogen cooling. The liquid hydrogen inlet manifold is located at the forward intake region near the cowl lip. The flow direction is aft toward the exit nozzle through tightly spaced cooling tubes embedded in the liner wall. The liquid hydrogen enters the inlet manifold at 2900 psi and at temperature of 57 °R. The total coolant mass flow rate is 24 Lbs/sec per engine. The cooling tube diameter is 0.16 inches and spaced 0.26 inches apart between tube centers. This will provide the necessary cooling for the liner and diverter pad, according to preliminary analyses. There will be high temperature insulation under the cowl aeroshell to keep the environmental heat from the flowpath heat exchanger.

The calculation of the engine component temperatures involves coupling a heat transfer model, fluid cooling model, and an engine cycle model together to solve the coupled conjugate heat transfer problem using SINDA/FLUINT and the Rocket Engine Transient Simulator (ROCETS), a propulsion cycle analysis code.[13] The ROCETS cycle code calculates the heat rate at the surface of the interior engine walls based upon an assumed hot wall temperature. This heat rate is then passed to the SINDA/FLUINT model to calculate a new hot wall temperature. The hot wall temperature is then passed back to the ROCETS cycle code to recalculate the hot wall heat rate. This iteration process is repeated until the hot gas wall temperature remains unchanged. The heat transfer coefficient used to calculate the heat rate is calculated using the Colburn Equation for the inlet, mixer/combustor, and nozzle region. For the rocket region, the Bartz equation is used to calculate the heat transfer coefficient. These calculations can only be run at a single Mach number in the trajectory. Using the one dimensional cycle analysis coupled with a thermal balance model, multiple runs were made for different Mach numbers along the trajectory to characterize the thermal profile. The maximum liner surface temperature was in the 1700 °R to 1800 °R temperature range. This is well within the maximum material temperature limit of the C/SiC material of 3460 °R.

In order to complete the characterization of the flowpath environment, both the internal engine temperatures and pressures were determined. The engine liner temperatures were computed using the methods already described. Internal engine pressures due to inlet compression, internal gas combustion, and exit nozzle expansion, were developed using other software packages including computational fluid dynamics and the Ramjet Performance Analysis code[14] for the critical ascent load cases.

INERTIAL AND PROPELLANT TANK PRESSURE LOADS

At liftoff, the tanks experience the inertia effects of 1.67 g, and this is the acceleration applied to the finite element model of the propellant tank stack. During acceleration the fluid structure interaction (pressure effects) must be modeled along with the mass effects. The resultant tank pressures must therefore be factored accordingly to account for inertia pressure effects. The height of the fluid decreases with consumption during flight as illustrated by Figure 13. At any given time, therefore, the tank pressure distributions are a function of fluid density, the height of the

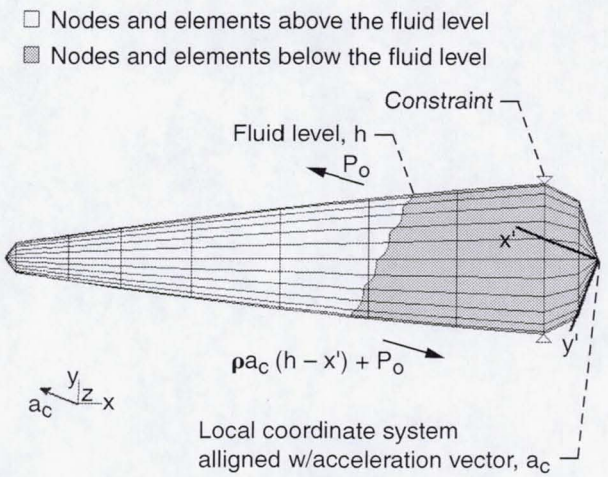

Figure 13.—LOX tank fluid pressure and inertia loading.

liquid propellant in each tank, and the angle of the acceleration vector with respect to the axis of the tank. From fluid statics, the pressure height relations can be used to determine the pressure equivalence down the tank.

$$P(x) = \rho g h(x) + p_0$$

Where: P is the tank pressure as a function of fluid height
p_0 is the nominal tank pressure (ullage)
h is the effective height of the fluid
g is the gravitational constant (or substitute acceleration, a_c)
ρ is the fluid density

The OTIS program calculates the amount of propellant remaining throughout the trajectory. OTIS also calculates the vehicle acceleration throughout the trajectory. A method was devised to determine the pressure equivalence at any time during flight. A finite element model of each tank was constructed and a local coordinate axis placed at the base was aligned with the acceleration vector, a_c. Next, the height of remaining propellant was calculated from an OTIS weight considering the volume occupied. Factored pressures are applied along the tank wall and the analysis is executed. The resultant at the base of the tank is then compared to the total acceleration force of the propellant mass plus the weight of the tank. This process was iterated, varying the height of the remaining fuel, until the resultant force versus resultant reaction matched to within one percent. A set of NASTRAN load cards was then generated from these results for each of the critical load cases to be included in the investigation as part of the static load set.

COMBINED LOADS ASSESSMENT AND OPTIMIZATION

At the completion of environment definition for each of the critical load cases, five separate NASTRAN™ run decks were prepared each having a thermal load set and a mechanical load set. The mechanical load set included aerodynamic pressures, inertia loads, propellant tank wall pressures and engine liner pressures. The thermal load set included mapped aero thermal loads on all structure, engine liner combustion wall temperatures, and cryogenic tank structure temperatures. Separate NASTRAN™ runs were executed for each of the five critical load cases using the static analysis solution. An output file was generated for each solution containing the member forces for each element in the integrated vehicle FEM. Similarly, for the detailed engine FEM, three critical load sets were applied with the appropriate thermal and pressure environment.

The NASTRAN output force files were imported into HyperSizer™ and combined for each of the critical load cases. HyperSizer™ calculated margins of safety using conventional formulas for failure criteria and selected the minimum margins from all possible flight events. Equivalent orthotropic plate properties were computed by creating ply lay-ups to maximize strength of composite sections. These composite properties were stored in the HyperSizer™ materials database for use in the component optimization process.

Structure systems in the integrated vehicle FEM, excluding the engine assembly, were then optimized for minimum weight using HyperSizer™. Similarly, the engine system components were optimized based on results of the detailed engine FEM. HyperSizer™ was used and supplemented by an in-house beam analysis code for engine cowl structure and this also served as a check of the optimizer results. Positive margins for all structure under the investigated loads were exhibited during the optimization process.

TABULATION OF SYSTEM WEIGHTS

The system dry weights for this structural assessment iteration are presented at a top level of assembly in Table 1. The dry weight total for this investigation of the integrated vehicle is 51,585 pounds. This compares to a dry weight total of 41,524 pounds as predicted by the spreadsheet for a 238,214 lb GLOW integrated vehicle. Systems exceeding the estimated weight are primarily in the area of vehicle thermal protection system (TPS), engine cowl and flow diverter structure, and the fuel delivery system. Weight growth beyond the original estimate is due in part to meeting structural requirements for the severe flight environment and also, to a more thorough design effort for the integrated system. The concepts for engine system architecture, for example, are well beyond the initial stages of design and development. This has been made possible through a partnership agreement with the Pratt & Whitney Company.

Table 1.—Comparison of Integrated System Dry Weight Predicted vs. Current Assessment

Assembly	Components	Original Estimate		Current Status	
		Weight (lbs)	Subtotal Weight (lbs)	Weight (lbs)	Subtotal Weight (lbs)
Aero-Shells			10675.5		10961.0
	Parabolic Nose Fairing	5418.6		5563.5	
	Midbody shell	2410.6		2475.1	
	Nozzle Shell	2846.3		2922.4	
TPS			1190.5		2618.1
	Parabolic Nose Fairing	571.4		802.0	
	LH2 Tank Cryogenics	537.5		1316.7	
	LOX Tank Cryogenics	81.5		499.4	
Tanks			5498.9		5568.3
	Liquid H2 tank	4199.1		3803.0	
	Liquid Ox tank	978.4		1000.0	
	Tank Adapter	321.4		765.3	
Wings			2992.4		2957.9
	Tail	735.0		821.5	
	Port wing	1128.7		1068.2	
	Starboard wing	1128.7		1068.2	
Payload			386.5		386.5
	Support	86.5		86.5	
	Cargo	300.0		300.0	
3 Engines			14847.2		21224.0
	Centerbodies	2090.5		2300.4	
	Cowls	7430.3		9635.0	
	Rockets	1994.8		859.8	
	Closeouts	1321.4		1365.9	
	Flow diverters	2010.3		7062.9	
Landing Gear			1997.3		1570.0
	Nose Gear	450.5		243.0	
	Main Gear	1546.8		1327.0	
Equipment			3935.7		6299.1
	AVTCS	492.2		476.0	
	ECLSS	170.8		165.2	
	EPD&C	668.1		668.1	
	Hydraulics	913.7		883.6	
	APU	226.7		219.2	
	RCS	165.4		159.9	
	VPP&D	225.2		217.8	
	Oxygen Delivery	597.2		984.8	
	Fuel Delivery	254.6		2310.0	
	Avionics (VMS)	221.8		214.5	
TOTAL	Vehicle (dry)		**41,524**		**51,585**

SUMMARY AND CONCLUSIONS

Using the results obtained from this assessment, the GTXSizer scaling code was updated with the new weight parameters. At the current size vehicle, the dry weight after vehicle assessment and optimization is approximately 24 percent high for closure. Although the vehicle dry weight total is above the prediction in this iteration, there are reasons for optimism in continuing development. The optimization, as performed, was focused on individual members in the current design rather than on strategic design modifications to save weight. For example, diverter pad support structure attaches to fuselage rings through built up sections. If fuselage rings were to be manufactured as one-piece members of varying depth, flanges and fasteners will be eliminated making a considerable weight savings. In addition, by varying spacing of rings and stringers to better accommodate structural loads, further weight could be saved. These and similar design improvements will lead to a more complete optimization of the integrated system. If this work is pursued further, it is expected that the margin of difference between estimated dry weight and the optimized structure would diminish significantly.

REFERENCES

1. FR–25292–1, GTX Structures/Materials/Thermal Management (SMTM), Trailblazer Rocket-Based Combined Cycle Propulsion System, Pratt & Whitney, West Palm Beach, FL, September 28, 2001.
2. Trefny, C.J.: An Air-Breathing Launch Vehicle Concept for Single-Stage-to-Orbit. AIAA Paper 99–2730, 1999.
3. Roche, J.M.; and McCurdy, D.R.: Preliminary Sizing of Vertical Take-Off Rocket-Based Combined-Cycle Powered Launch Vehicles, NASA/TM—2001-210668, January 2001.
4. Hargraves, C.R.; and Paris, S.W.: Direct Trajectory Optimization Using Non-Linear Programming and Collocation, Journal of Guidance Control and Dynamics, Vol. 10, No. 4, p. 338, July-August 1987.
5. Roskam, Jan: Airplane Design. Part 5-Component Weight Estimation. Roskam Aviation and Engineering Corp., Ottawa, KS, 1989.
6. Pro/ENGINEER®, Parametric Technology Corporation, Needham, Massachusetts, Version 2000.
7. Bonner, E.; Clever, W.; and Dunn, K.: Aerodynamic Preliminary Analysis System II, Part I–Theory, 1989.
8. MSC/PATRAN™, The MacNeal-Schwendler Corporation, Los Angeles, CA, Version 2000.
9. MSC/NASTRAN™, The MacNeal-Schwendler Corporation, Los Angeles, CA, Version 70.
10. HyperSizer™ Structural Sizing Software, Third Ed., Collier Research and Development Corporation, Hampton, VA, 1998.
11. SINDA/FLUINT, General Purpose Thermal/Fluid Network Analyzer, Version 4.3, Cullimore and Ring Technologies, Inc., June 2000.
12. Engel, C.D.; and Praharaj, S.C.: MINIVER Upgrade for the AVID System, Volumes 1–3, NASA Contractor Report, Contract NAS1–16983, REMTECH, Inc., Huntsville, AL, August 1983.
13. ROCETS, Rocket Engine Transient Simulation, Pratt & Whitney Company, West Palm Beach, FL, 1991.
14. Pandolfini, P.P.; and Friedman, M.A.: Instructions for Using Ramjet Performance Analysis RJPA IBM-PC Version 1.24. The Johns Hopkins University Applied Physics Laboratory, JHU/APL AL–92–P175, June 1992.

ACKNOWLEDGMENTS

The authors would like to thank the members of the GTX project, research, and engineering team at the NASA Glenn Research Center for their contribution to this paper: Don Palac, Chuck Trefny, Joe Roche, Jim Yuko, David Myers, Tom Niezgoda, Miguel Polanco, John Riehl, and John Ramsey, NASA, Reza Zinolabedini and Jim Davic, QSS Group, Inc., and Dan Kosareo, Zin Technologies.